

Thermal stability of magnetron sputtering Ge-Ga-S films

Lei Niu(牛磊), Yimin Chen(陈益敏), Xiang Shen(沈祥), Tiefeng Xu(徐铁峰)
Citation: Chin. Phys. B . 2020, 29(8): 087803 . **doi:** 10.1088/1674-1056/aba273
Journal homepage: http://cpb.iphy.ac.cn; http://iopscience.iop.org/cpb

What follows is a list of articles you may be interested in

Refractive index of ionic liquids under electric field: Methyl propyl imidazole iodide and several derivatives

Ji Zhou(周吉), Shi-Kui Dong(董士奎), Zhi-Hong He(贺志宏), Yan-Hu Zhang(张彦虎)
Chin. Phys. B . 2020, 29(4): 047801 . **doi:** 10.1088/1674-1056/ab75cd

High-performance lens antenna using high refractive index metamaterials

Lai-Jun Wang(王来军), Qiao-Hong Chen(陈巧红), Fa-Long Yu(余发龙), Xi Gao(高喜)
Chin. Phys. B . 2018, 27(8): 087802 . **doi:** 10.1088/1674-1056/27/8/087802

Accuracy design of ultra-low residual reflection coatingsfor laser optics

Huasong Liu(刘华松), Xiao Yang(杨霄), Lishuan Wang(王利栓), Hongfei Jiao(焦宏飞), Yiqin Ji(季一勤), Feng Zhang(张锋), D an Liu(刘丹丹), Chenghui Jiang(姜承慧), Yugang Jiang(姜玉刚), Deying Chen(陈德应)
Chin. Phys. B . 2017, 26(7): 077801 . **doi:** 10.1088/1674-1056/26/7/077801

Nonlinear optical characterization of phosphate glasses based on ZnO using the Z-scan technique

Masoumeh Shokati Mojdehi, Wan Mahmood Mat Yunus, Khor Shing Fhan, Zainal Abidin Talib, N. Tamchek
Chin. Phys. B . 2013, 22(11): 117802 . **doi:** 10.1088/1674-1056/22/11/117802

Optical study of $Ba(Mn_xTi_{(1-x)}O_3)$ thin films by spectroscopic ellipsometry

Zhang Ting, Yin Jiang, Ding Ling-Hong, Zhang Wei-Feng
Chin. Phys. B . 2013, 22(11): 117801 . **doi:** 10.1088/1674-1056/22/11/117801

Thermal stability of magnetron sputtering Ge–Ga–S films*

Lei Niu(牛磊)[1], Yimin Chen(陈益敏)[1,2,†], Xiang Shen(沈祥)[1,‡], and Tiefeng Xu(徐铁峰)[1]

[1] *Laboratory of Infrared Materials and Devices & Key Laboratory of Photoelectric Detection Materials and Devices of Zhejiang Province, Research Institute of Advanced Technology, Ningbo University, Ningbo* 315211, *China*

[2] *Department of Microelectronic Science and Engineering, School of Physical Science and Technology, Ningbo University, Ningbo* 315211, *China*

(Received 10 April 2020; revised manuscript received 17 June 2020; accepted manuscript online 3 July 2020)

Ge–Ga–S thin films were deposited by magnetron sputtering with mean coordination number (MCN) ranging from 2.46 to 2.94. The physical properties of the Ge–Ga–S films, including optical band gap, refractive index, and thickness, vary with the time of heat treatment. Based on the analysis of the topology model, it is concluded that the Ge–Ga–S thin films with components close to the stoichiometric ratio can form the most Ga–S bonds and Ga–S bonds, and the physical properties of the $Ge_{27.3}Ga_{6.3}S_{66.3}$ (MCN = 2.62) film are the most stable. This is an important reference for thin film photonic devices.

Keywords: chalcogenide thin films, refractive index, optical band gap, thermal stability

PACS: 78.20.Ci, 78.40.Fy, 78.40.−q **DOI:** 10.1088/1674-1056/aba273

1. Introduction

Chalcogenide glasses are important amorphous materials, which have good transparency in the infrared region[1] and high linear[2] and nonlinear refractive indexes.[3] They are widely used in the field of infrared optics,[4] including optical waveguide,[5] optical fiber, all-optical switching,[6] etc. Sulfur-based films can be used to prepare non-linear optical devices,[7] optical chips, infrared lasers,[8] etc. For many applications, the preparation of high quality optical thin films with stable physical properties is an essential step in device manufacturing. As we all know, when materials are exposed to light, heat, etc, even in the bulk of the amorphous semiconductor (such as chalcogenide) chemical bonds will relax,[9] which will lead to changes in physical properties (such as band gap and energy band), resulting in changes or degradation in the performance of the manufactured devices.[10] Therefore, photo or thermally induced changes in chalcogenides have been the subject of extensive research. Optical band gap and refractive index, two basic optical parameters, unusually change with the external energy input in chalcogenide glasses.

The physical properties of chalcogenide glasses are not only closely related to the glass structure, but also to the mean coordination number (MCN) as proposed by Phillips.[11] MCN is the sum of the concentration of each element multiplied by their covalent coordination number. The characteristics of covalent glass network are explained by the theory of constraint counting. Phillips pointed out that for a three-dimensional covalent network, when MCN = 2.4, the best conditions for forming a three-dimensional glass network can be formed. Thorpe's[12] further development adopts the concept of rigid permeation applied to covalent chalcogenides. When MCN is less than 2.4, the network structure is flexible, when MCN is more than 2.4, the network structure is over-constrained and the stress is rigid. Later, Tanaka[13] studied the composition dependence of the structure, elasticity, and electronic properties of chalcogenide glasses, indicating that additional structural phase transition would occur at MCN = 2.67, from the two-dimensional structure of materials with MCN $\leq$ 2.67 to the three-dimensional structure of materials with MCN>2.67. More and more experimental evidences show that under these MCN values,[14] many chemical and physical properties exhibit threshold behaviors.

In this work, we have prepared seven Ge–Ga–S films with different compositions by magnetron sputtering. The composition range of the compounds is from MCN = 2.46 to MCN = 2.94. The evolution of optical properties of these films after thermal annealing at glass transition temperature has been studied. The films are annealed in a vacuum oven to minimize oxidation on the sample surface. Thermal stability of the Ge–Ga–S thin films is investigated in a relatively wide composition range. The purpose is to find the compounds with the most stable optical properties after annealing, and to explore the relationship between MCN value and the degree of band gap and refractive index changes.[15]

2. Experimental details

$Ge_xGa_7S_{93-x}$ glasses were prepared using conventional melt-quenching technology, with a composition range of x

*Project supported by the National Natural Science Foundation of China (Grant Nos. 61675105, 61775111, and 61904091), Ningbo Optoelectronic Materials and Devices Laboratory (Grant No. 2009B21007), and K. C. Wong Magna Fund in Ningbo University of China.

†Corresponding author. E-mail: chenyimin@nbu.edu.cn

‡Corresponding author. E-mail: shenxiang@nbu.edu.cn

© 2020 Chinese Physical Society and IOP Publishing Ltd

from 20 to 45. The as-prepared glasses with a diameter of 50 mm and a thickness of 3.5 mm were polished and then bonded onto a copper sheet for sputtering. The films with different components were thus prepared on thermally-oxidized silicon and quartz wafers.

The glass transition temperature of each glass was measured by DSC. At the glass transition temperature of 20 °C, the corresponding films were annealed in a vacuum oven for various durations. For the annealing process, we first put the Ge–Ga–S film into the oven, and vacuumed it for more than half an hour with a mechanical pump. Then, we heated up the film to the target temperature with a heating rate of 1 °C/min, and maintained this temperature for 1 h, 3 h, 5 h, 15 h, 30 h. Finally, we cooled down the sample to the room temperature with the cooling rate of 1 °C/min.

The film compositions were measured using energy dispersive x-ray analysis (EDX). A conventional x-ray diffractometer was used to check the amorphous properties of the film. Optical band-gap energy (E_g) was measured by an UV–visible–near-infrared spectrometer (Perkinelmer lambda 950), and the refractive index (n) and thickness of the film were measured by (IR-Vase Mark 2) variable-incident angle infrared spectral type elliptic polarization instrument. The composition, thickness, and corresponding MCN values of the film are listed in Table 1.

Table 1. Composition, MCN, and thickness of Ge–Ga–S deposited film.

Film composition (Ge/Ga/S)	Film MCN	Film thickness/nm
20.0/6.5/74.5	2.46	351
22.5/8.1/69.4	2.53	344
27.4/7.3/65.3	2.62	507
30.4/8.4/61.2	2.69	289
33.1/7.9/59.0	2.74	242
38.5/8.4/53.1	2.85	450
43.6/6.8/49.6	2.94	488

3. Results and discussion

The ellipticity parameter amplitude ratio (Ψ) and phase difference (Δ) of the thin film are measured with the infrared ellipsometer.[16] The measurement angles are 65° and 75°. Two optical models of silicon dioxide substrate layer and thin film layer are established. Then the fitting results are made with the IR-VASE software. The Cauchy dispersion model is selected for the thin film layer. The Cauchy dispersion relationship is more suitable for most thin films with weak absorption or transparency, which can match many films well. The error of the fitting results can be measured by mean square error (MSE). One of the film fitting results is shown in Fig. 1, which is consistent with the experimental value, MSE is 1.9. The cliff jump of the curve in Fig. 1(b) is caused by the change of the P light (parallel to the incident plane polarization) disappearing position. The film thickness can be obtained by fitting. The fitting parameters A, B, C and refractive index can be obtained by Cauchy formula

$$n(\lambda) = A + B/\lambda^2 + C/\lambda^2. \tag{1}$$

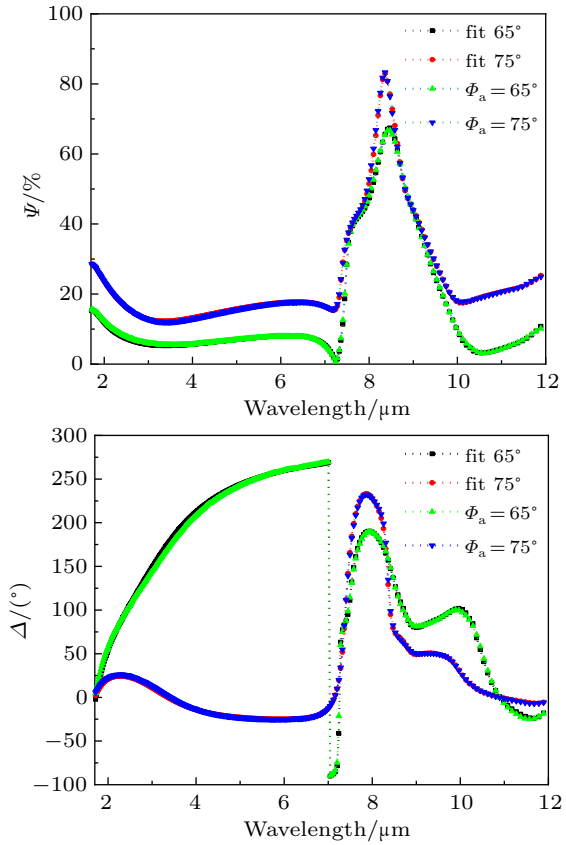


Fig. 1. Fitting results of Ψ and Δ for fresh $Ge_{27.4}Ga_{7.3}S_{65.3}$ film by the Cauchy model. Two test angles (65° and 75°) are employed here.

The refractive index of the deposited films as a function of MCN is shown in Fig. 2. Generally, the refractive index increases with increasing MCN, except at a narrow range of $2.62 \leq \text{MCN} \leq 2.69$, where the evolution of the refractive index exhibits a dip with a minimum value of 1.94 at MCN = 2.62. This could be due to the transition of the network from 2D rigidity to 3D stress-rigidity at MCN ~ 2.67.

According to the Lorentz–Lorenz relationship,[17] the refractive index is related to the density of polarizable units, which can be expressed as

$$\frac{n^2-1}{n^2+2} = \frac{4\pi}{3}\sum_i N_i \alpha_{\mathrm{p},i}, \tag{2}$$

where $\alpha_{\mathrm{p},i,}$ is the electronic polarizability and N_i is the number of polarizable units of type i per volume unit. Since the atomic weight and polarizability of Ge are larger than those of S, the increase of the refractive index in films with increasing Ge content (and thus increasing MCN) in Fig. 1 is due to the increase of the density and polarizability of the films.

Figure 3 is the variation of the refractive index as a function of the annealing time for the films with different compositions. It can be clearly seen that the evolution of the refractive

index of the films shows different behaviors. For the compound with $2.46 \leq \text{MCN} \leq 2.62$ (S rich region), the refractive index increases with the increase of annealing time, and the smaller the MCN value, the greater the refractive index change. For the compound with $2.69 \leq \text{MCN} \leq 2.94$ (S deficient region), the refractive index decreases with the increase of annealing time, and the larger the MCN value, the greater the refractive index change.

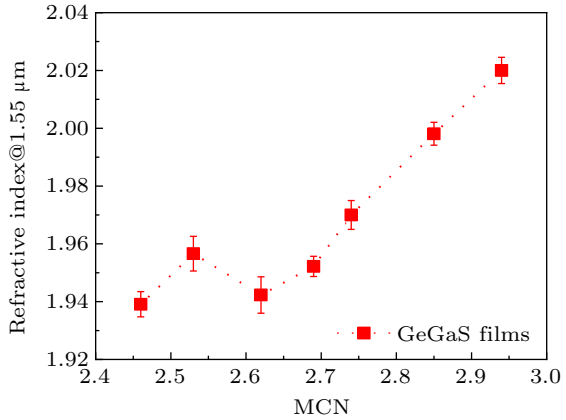


Fig. 2. Linear refractive index at 1550 nm wavelength for the as-deposited films as a function of MCN.

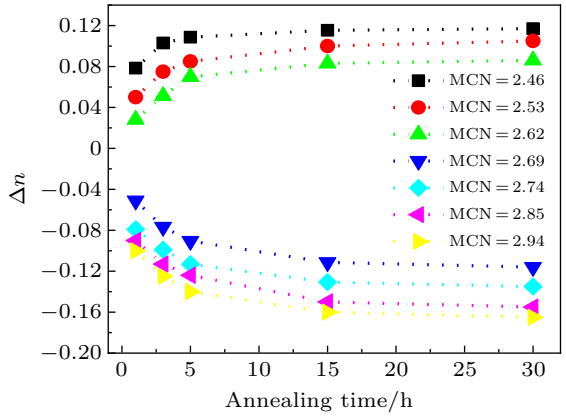


Fig. 3. The relationship between refractive index variation of Ge–Ga–S film and annealing time.

When the film is deposited under thermodynamic inequilibrium conditions, more wrong or defective bonds can be induced in the films compared with the bulk glass that is prepared under thermodynamic equilibrium conditions, these defective bonds can be rearranged upon thermal annealing, resulting in a larger refractive index variation of the film. For the intermediate MCN value, the refractive index difference before and after annealing is very small. In fact, this suggests that the films may have fewer defective bonds.

Tauc model is used to calculate the optical band gap of thin films

$$\alpha h\nu = B(h\nu - E_{\mathrm{g}})^2, \tag{3}$$

where E_{g} is the band gap energy, B is the slope of the Tauc side, $h\nu$ is the photon energy, and h is a constant.

The E_{g} value of the as-deposited film decreases with the increase of MCN which is evident in Fig. 4. However, when MCN = 2.62 around the stoichiometric ratio, their band gap value slightly increases, it can be explained by that more Ga–S bonds and Ga–S bonds are formed at this time, and the average bond energy is larger, in agreement with the classical oscillator model for the dielectric constant in semiconductors[18] for which $1/(n^2-1)$ is proportional to E_{g}^2.[19]

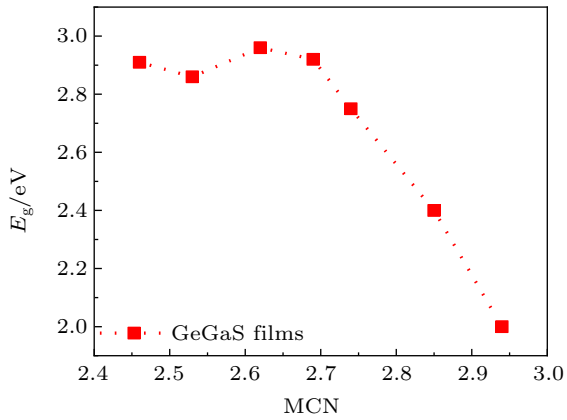


Fig. 4. Optical band-gap energy for as-deposited films as a function of MCN.

The effect of annealing time on E_{g} is illustrated in Fig. 5. The evolution of the band gap is obviously divided into two groups. At $2.46 \leq \text{MCN} \leq 2.62$ (S-rich region), the band gap decreases after annealing, while at $2.69 \leq \text{MCN} \leq 2.94$ (S-deficient region), the band gap increases after annealing, and the change amount of the band gap increases with the annealing time. At intermediate MCN value, the change in band gap is the least. this can be explained as follows: when the chemical composition of the region is closer to the stoichiometric composition, the wrong bond is less likely to occur. According to Mott and Davies model, the disorder degree of high MCN and low MCN films prepared under non-equilibrium condition is higher, so the change of optical band gap caused by annealing is more obvious. Here, the film with MCN = 2.62 has the best stability.

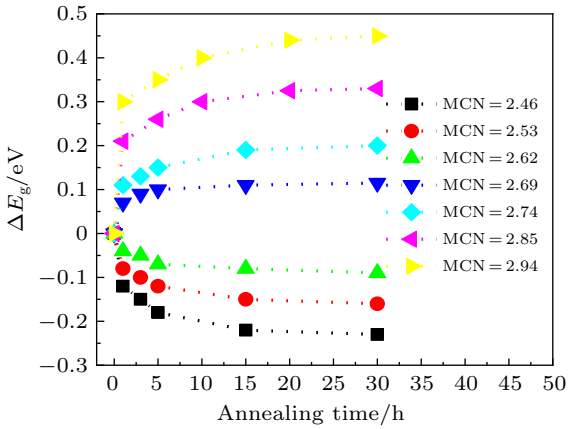


Fig. 5. Relationship between optical band-gap variation and annealing time of Ge–Ga–S films.

The thickness of the films changes after annealing. The film thickness ratio $\Delta d/d$ is defined as: (annealed minus as-deposited) divided by as-deposited. The Ge–Ga–S film thickness ratio is shown in Fig. 6. After the heat treatment, the thickness of the film is reduced, and the longer the annealing time is, the more the film decreases, and finally becomes stable. Consistent with the changes of band gap and refractive index in front, the film with MCN = 2.69 has the smallest thickness change. It indicates that the low MCN and high MCN films have greater disorder and instability. The film with intermediate MCN has the best thermal stability.

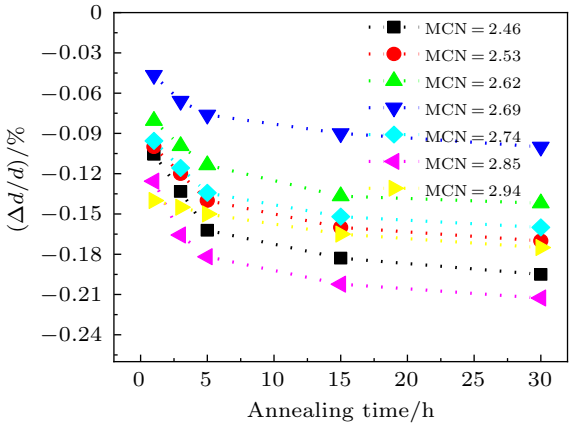


Fig. 6. Film thickness variation as a function of annealing time.

4. Conclusions

In summary, seven Ge–Ga–S films with different components were prepared by magnetron sputtering from Ge–Ga–S bulk glass. After annealing, it can be seen that the evolutions of optical band gap and refractive index of the films are divided into two different regions. At $2.46 \leq \text{MCN} \leq 2.62$ (rich S region), the band gap of the film red-shifted and the refractive index gradually increased with the increase of annealing time. At $2.69 \leq \text{MCN} \leq 2.94$ (deficient S region), the band gap blue-shifted and refractive index decreased with the increase of annealing time. Among them, when MCN = 2.62, the optical band gap, refractive index, and thickness of the film had the smallest change with annealing time. Therefore, it is found that the component of $Ge_{27.4}Ga_{6.3}S_{66.3}$ has the best thermal stability. In addition, according to Tanaka,[13] the second phase transition existed at MCN = 2.67, which represents the topological change from 2D to 3D "stress-rigid" phase. The experimental results in this paper show that the turning point is near MCN $\sim$ 2.67, which also verifies the topological theory to some extent. Finally, we believe that the preparation of thin films under thermodynamic unbalance conditions (magnetron sputtering, thermal evaporation, etc.) can reduce the wrong bonds and defects in the films when the components are close to their stoichiometric ratios, thus forming films with good thermal stability.

References

[1] Zhu E W, Zhao X H, Wang J S and Lin C G 2018 *J. Non-Cryst. Solids* **489** 45
[2] Musgraves J D, Carlie N, Hu J, Petit L, Agarwal A, Kimerling L C and Richardson K A 2011 *Acta Mater.* **59** 5032
[3] Wang T, Gai X, Wei W H, Wang R P, Yang Z Y, Shen X, Madden S and Luther-Davies B 2014 *Optical Materials Express* **4** 1011
[4] Li C R, Dai S X, Zhang Q Y, Shen X, Wang X S, Zhang P Q, Lu L W, Wu Y H and Lv S Q 2015 *Chin. Phys. B* **24** 044208
[5] Yan K L, Vu K, Yang Z Y, Wang R P, Debbarma S, Luther-Davies B and Madden S 2014 *Optical Materials Express* **4** 464
[6] Zakery A and Elliott S R 2003 *J. Non-Cryst. Solids* **330** 1
[7] Chu S S, Wang S F, Tao H Z, Wang Z W, Yang H, Lin C G, Gong Q H and Zhao X J 2007 *Chin. Phys. Lett.* **24** 727
[8] Zhang M J, Yang A P, Peng Y F, Zhang B, Ren H, Guo W, Yang Y, Zhai C C, Wang Y W, Yang Z Y and Tang D Y 2015 *Materials Research Bulletin* **70** 55
[9] Wang R P, Madden S J, Zha C J, Rode A V and Luther-Davies B 2006 *J. Appl. Phys.* **100** 063524
[10] Wang R P, Choi D Y, Rode A V, Madden S J and Luther-Davies B 2007 *J. Appl. Phys.* **101** 113517
[11] Phillips J C 1979 *J. Non-Cryst. Solids* **34** 153
[12] Thorpe M F 1983 *J. Non-Cryst. Solids* **57** 355
[13] Tanaka, Saito, Suzuki and Hasegawa 1985 *Phys. Rev. B* **32** 6853
[14] Kamitakahara, Cappelletti, Boolchand, Halfpap, Gompf, Neumann and Mutka 1991 *Phys. Rev. B* **44** 94
[15] Bulla D A P, Wang R P, Prasad A, Rode A V, Madden S J and Luther-Davies B 2009 *Appl. Phys. A* **96** 615
[16] Wei N N, Yang Z, Pan H B, Zhang F, Liu Y X, Wang R P, Shen X, Dai S X and Nie Q H 2018 *Chin. Phys. B* **27** 067802
[17] Jackson J D 1999 *Physics Today* **52** 78
[18] Ravindra N M, Ganapathy P and Choi J 2007 *Infrared Physics & Technology* **50** 21
[19] Hervé P and Vandamme L K J 1994 *Infrared Physics and Technology* **35** 609